Searching For p+ p+ Rapidity Dependent Correlations in Ultra-relativistic Quantum Molecular Data

Isaac Pawling

(Dated: August 7, 2015)

Abstract

Finding rapidity dependent particle correlations in particle distributions from heavy-ion collisions could be indicative of a state with increased correlation length. A divergence of the correlation length could indicate the location of a critical point on the QCD phase diagram and a first order phase transition. This paper will outline the study of an algorithm used to look through events in Ultra-relativistic Quantum Molecular Dynamics (UrQMD) for these relationships by calculating the two particle correlation variable R_2 as a function of rapidity. The algorithm was written and tested using the ROOT data analysis framework. Tests were performed using randomly generated data which revealed the need to introduce a correction to the calculation. This algorithm has the potential to be applied to other data models and is eventually aimed at data from the Solenoidal Tracker At RHIC (the Relativistic Heavy-ion Collider).

I. PURPOSE OR MOTIVATION

The Relativistic Heavy-ion Collider accelerates two particle beams in opposite directions inside a pipe. Located at beam intersection points around the collider are particle detectors which allow scientists to gather data on small-scale high-energy phenomena. RHIC has the ability to accelerate particles as large as gold nuclei to those as small as protons. The beam energies at RHIC range from 7.7 to 200 GeV. The Solenoidal Tracker At RHIC (STAR) is a detector that provides useful momentum measurements of particles that are created after a collision. From these momentum measurements, the rapidity can be calculated.

Particle correlations as a function of rapidity are being studied in an attempt to locate the possible critical point on the quantum chromodynamic (QCD) phase diagram which is shown in Figure 1. At low temperatures, nuclear matter takes the form of hadrons. High temperatures cause hadrons' constituent quarks to become deconfined and a state of matter called quark gluon plasma (QGP) is formed. The first order phase transition and critical point on this plot are speculative. The critical point can be identified by a divergence in the correlation length. In this state, nuclear matter on the QCD phase diagram would consist of distinct and large domains of hadrons and guark-gluon plasma (QGP). Crossing the first order phase transition would cause some change in a state variable. On this diagram is also a region of cross-over phase transition (the dotted line) that involves no change in a state variable.

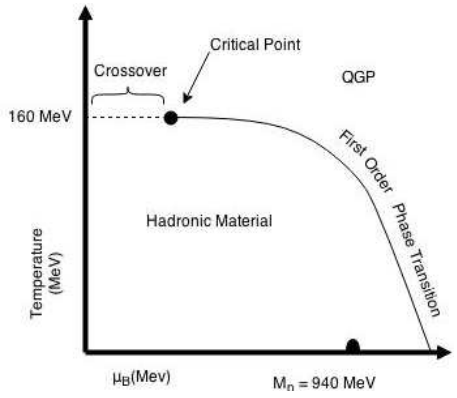

FIG. 1: The quantum chromodynamic phase diagram. On the horizontal axis is the baryochemical potential, μ_B, and the vertical axis is the temperature, T. Both axes are in MeV. Located at the 940 MeV is the mass of a proton.

The purpose of this project is to write a program that will analyze data and look for

rapidity dependent two-particle correlations in the top 5% most central, or "head on," Au+Au collisions. The program will be tested using UrQMD data, with the ultimate goal of searching for this type of correlation in data from the STAR detector. Finding increased two particle correlations would indicate a state of matter where compared particles are traveling in a correlated manner.

II. VARIABLES

Collisions are defined by an impact parameter b which ranges from zero to twice the radius of the Au nucleus. An impact parameter of 0 is the most head-on collision, and a b value of 2R is the most peripheral collision. In a central heavy-ion collision, the matter becomes ultra-dense and super-heated. The intense pressure and heat available in the system causes the matter (QGP) to expand rapidly. This expansion is accompanied by the matter cooling down, hadronizing, and ceasing strong interactions. This phase is called freeze-out and the particles then stream out to the detector.

In high-energy nuclear physics, 3-vector momentum is measured with the z-axis parallel to the the beam axis. Rapidity y, is a relativistic alternative to angle with respect to the beam axis. It is given by:

$$y = \frac{1}{2} ln \frac{E + p_z}{E - p_z}, \tag{1}$$

where E is the particle's energy, and p_z is the component of the particle's momentum in the z-direction [2].

The two particle correlation function, R_2, is defined as,

$$R_2 = \frac{C_2(y_1, y_2)}{\rho_1(y_1)\rho_1(y_2)}. \tag{2}$$

R_2 is derived from C_2 (Equation 3) which is the cumulant correlation function [1]. y_1 and y_2 are the respective particle rapidities being compared and $\rho_1(y_1)\rho_1(y_2)$ is a 2D histogram defined as the tensor product of the 1D rapidity distribution over events. C_2 is defined as

$$C_2 = \rho_2(y_1, y_2) - \rho_1(y_1)\rho_1(y_2), \tag{3}$$

where $\rho_2(y_1, y_2)$ is a 2D histogram called the rapidity pair distribution.

R_2 can be rewritten as

$$R_2 = \frac{\rho_2(y_1, y_2) - \rho_1(y_1)\rho_1(y_2)}{\rho_1(y_1)\rho_1(y_2)} = \frac{\rho_2(y_1, y_2)}{\rho_1(y_1)\rho_1(y_2)} - 1. \tag{4}$$

R_2 is a measure of correlation; the observable is designed to be equal to zero for uncorrelated data, be positive for positively correlated data, and be negative for anti-correlated data [1].

III. PROCEDURE

The majority of my research consisted of coding in a language developed by the European Organization for Nuclear Research (CERN) called ROOT. ROOT is a data analysis framework in the C++ class library.

To create R_2, first a 1-D rapidity distribution is created. This histogram is filled with the number of particles with a rapidity less than 1 and greater than -1. Figure 2 gives some examples of rapidity distributions measured by different experiments. These rapidity values are also stored in an array which is cleared before each event. After each event, a 2-D histogram $\rho_2(y_1, y_2)$ is filled with non-self rapidity pairs whose values are retrieved from the previously referenced array. After all events have been analyzed, $\rho_2(y_1, y_2)$ is then normalized by the number of events.

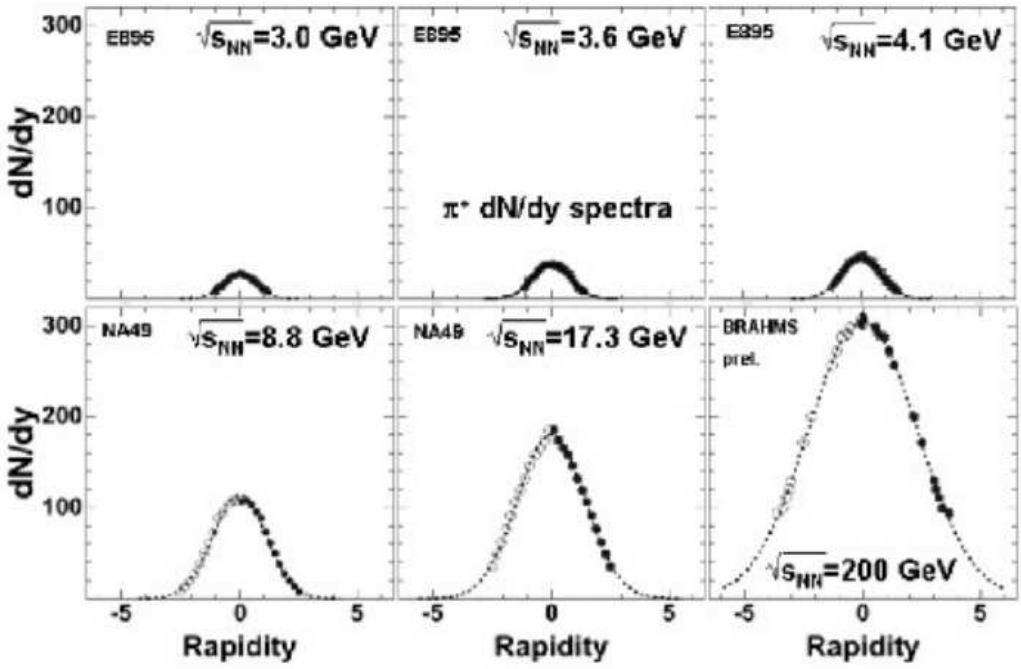

FIG. 2: Rapidity distributions for various energies [1]

To produce the other histogram needed to calculate R_2, the 1-D histogram (rapidity distribution) filled above is used in a double-nested loop. This is used to calculate the

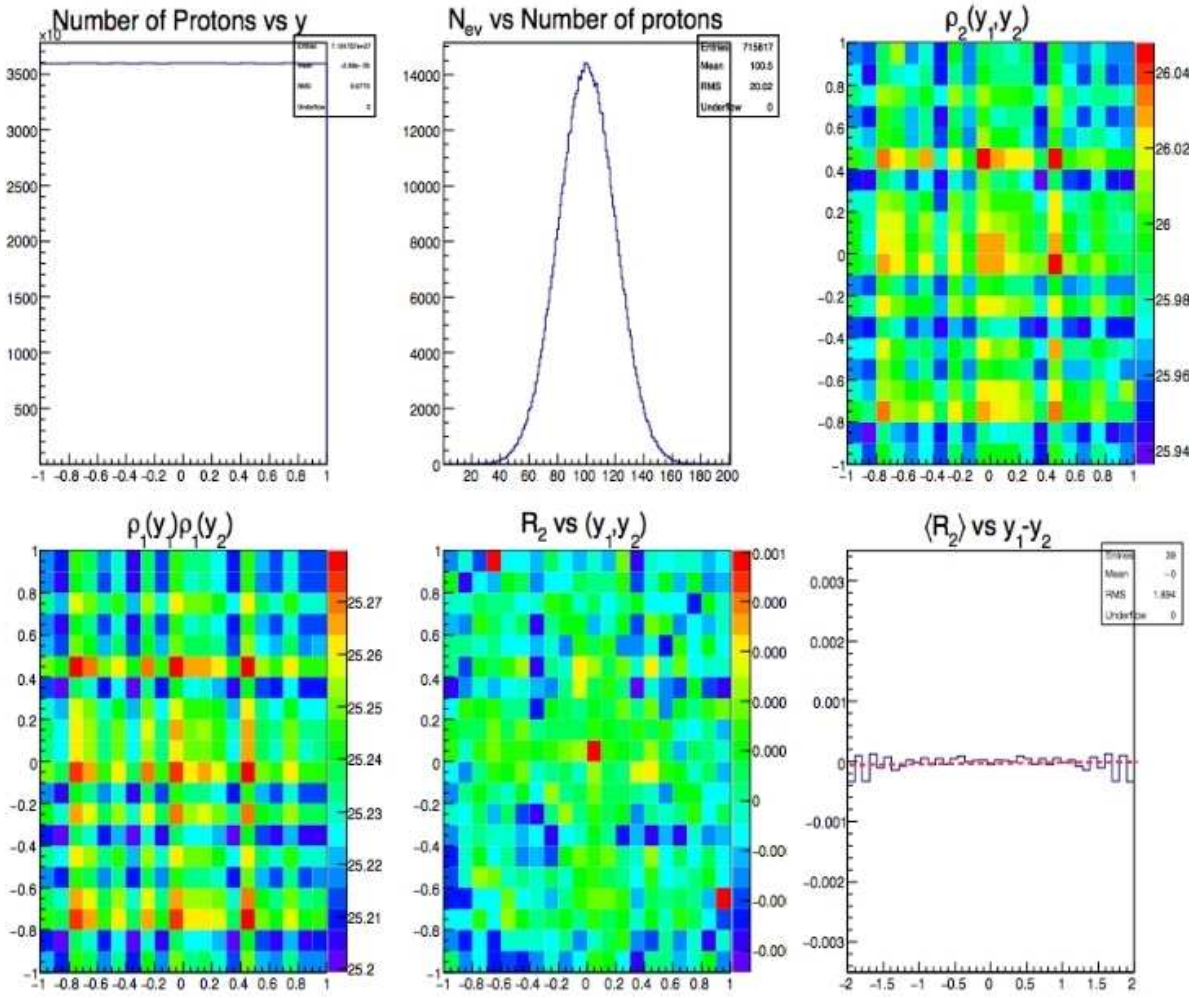

FIG. 3: Plots produced using random data. Note the small range on the z-axis for the 2D histograms. These histograms are essentially flat.

tensor product of the rapidity distribution which is another 2-D histogram $\rho_1(y_1)\rho_1(y_2)$. Each loop runs over the entire 1-D histogram, and all bins are compared the same number of times so this plot is symmetric about the line $y_1 = y_2$.

R_2 is calculated by taking the ratio of the two histograms, $\frac{\rho_2(y_1,y_2)}{\rho_1(y_1)\rho_1(y_2)}$, and subtracting 1 from each bin. Examples of the rapidity pair distribution and the tensor product of the rapidity distribution can be seen in Figure 3.

Since R_2 is symmetrical about the line $y_1 = y_2$, average values are calculated along the diagonal. The number of bins, difference in rapidity values, and total entries in each diagonal row are totaled. The entries are averaged over the number of bins in each diagonal. These averaged entries are then used to fill a 1-D histogram as a function of the average difference

in rapidity. This histogram is $\langle R_2 \rangle$ as a function of Δy. Figure 4 shows gives a graphical depiction of this procedure.

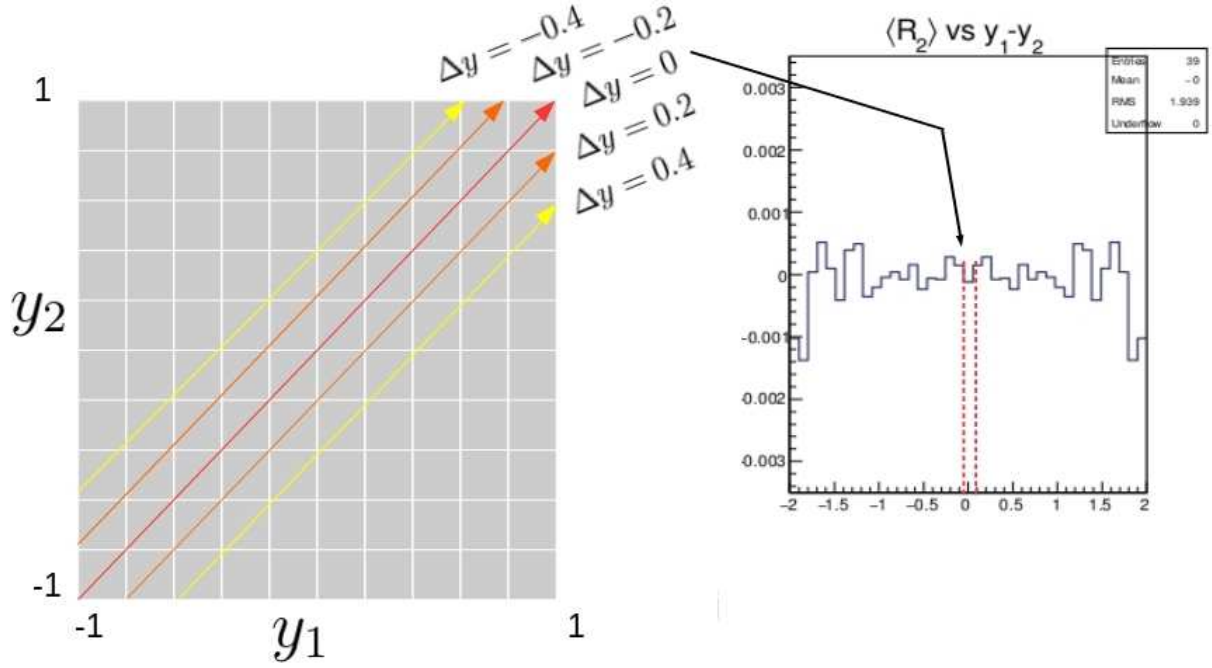

FIG. 4: $\langle R_2 \rangle$ vs dy is symmetrical by construction

Initial calculations for $\langle R_2 \rangle$ used a fixed number of particles per event and random rapidity values. Although a $\langle R_2 \rangle$ of 0 was expected, a non-zero value was calculated. Pairs of equally probable number of particles per event as well as small ranges of possible N_{part}/evt were also tested using the random rapidity values. These $\langle R_2 \rangle$ values were also non-zero. Table 1 shows the tested number of particles per event and the $\langle R_2 \rangle$ value. It was concluded that because the number of particles per event is small, a correction needs to be introduced to account for offset due to finite counting statistics. This was corrected by subtracting a baseline R_2 value, R_2^{bs}, that accounts for the N_{part} bias. The baseline value was determined to be [1]:

$$R_2^{bs} = \frac{\langle n(n-1) \rangle}{\langle n \rangle^2} - 1 = \frac{\sum y_i * n_i * (n_i - 1)}{(\sum n_i * y_i)^2} - 1, \tag{5}$$

where n_i is the i-th N_{part} per event, y_i is the counted number of n_i's with the normalization $\sum y_i = 1$. For the following studies, the values of R_2^{bs} at fixed n from equation (5) are averaged over the multiplicity distributions in given event samples to correct for the finite counting offsets.

N_{part}	$\langle R_2 \rangle$	N_{part}	$\langle R_2 \rangle$
2,3	-1/3	2,6	0
3,4	-1/4	4,6	-1/6
4,5	-1/5	3,6	-1/9
5	-1/5	1,6	+.225
2-6	-1/6	10-14	-1/14

TABLE I: Calculated values of $\langle R_2 \rangle$ for equally probably fixed N_{part}

IV. RESULTS

Figure 5 is a typical page of plots produced by the code run over central collisions at a beam energy of 7.7 GeV. This plot shows a clear signal for $\langle R_2 \rangle - R_2^{bs}$ vs the difference in rapidity. There is a slightly increased probability of finding a proton pair with a difference in rapidity of about 0.8, and slightly decreased probability for finding a proton pair with a difference in rapidity of 0 or 2.

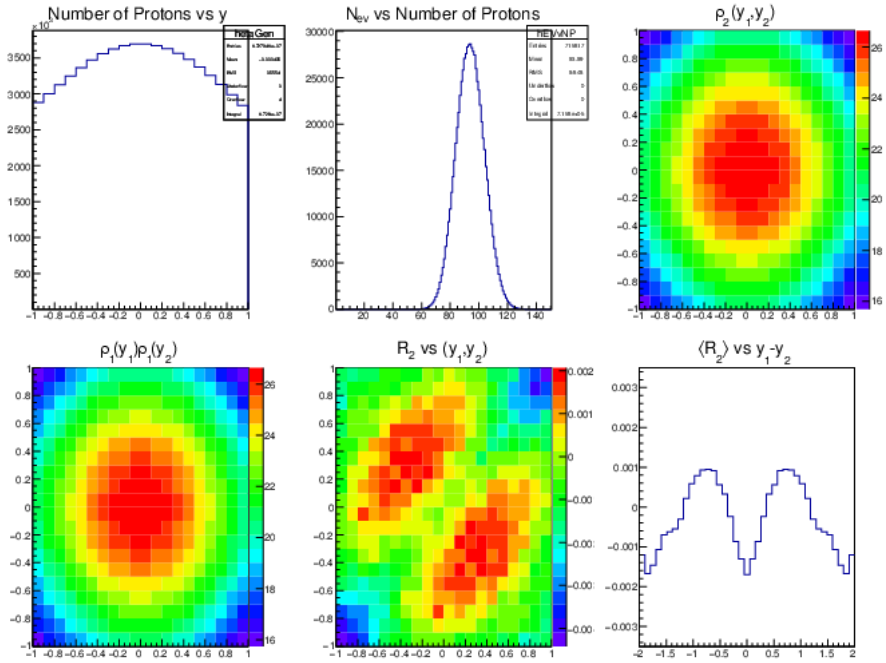

FIG. 5: Example plot: from UrQMD data set 19 (7.7 GeV)

The averaged $\langle R_2 \rangle - R_2^{bs}$ values as a function of Δy are given by Figure 6. These values have been calculated for beam energies 7.7, 11.5, 14.5, 19.6, 27, 39, 62.4, and 200 GeV. The lower energy $\langle R_2 \rangle - R_2^{bs}$ plots have a clear correlation signal at dy$\sim$0.8 that diminishes as the beam energy is increased.

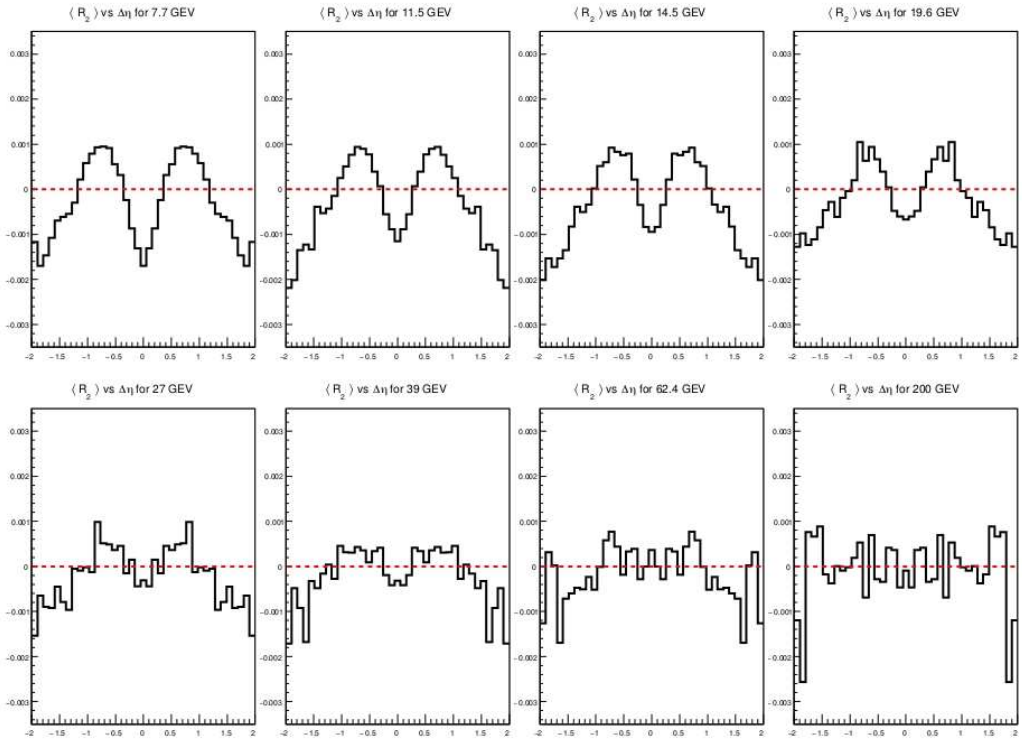

FIG. 6: $\langle R_2 \rangle - R_2^{bs}$ for 8 energy levels (increasing energy left to right, top to bottom)

The next figure was produced in an attempt to understand how the distributions of both rapidity and the number of of protons per event effects the $\langle R_2 \rangle - R_2^{bs}$ values. Figure 7 shows a $\langle R_2 \rangle - R_2^{bs}$ calculation using rapidity values sampled from a flat distribution and number of particles per event sampled from the UrQMD N_{part}/evt distribution. This portion of the figure (the upper row) shows what is expected when using random rapidity values. The $\langle R_2 \rangle - R_2^{bs}$ plot shows no correlations when uncorrelated rapidity values are used. Figure 7 also shows a $\langle R_2 \rangle - R_2^{bs}$ calculation using rapidity values sampled from both the UrQMD $Npart/evt$ and y distributions. This part of the figure (the bottom row) shows that R_2 is dependent on the intra-event particle rapidities, rather than being dependent on the rapidity distribution over all events.

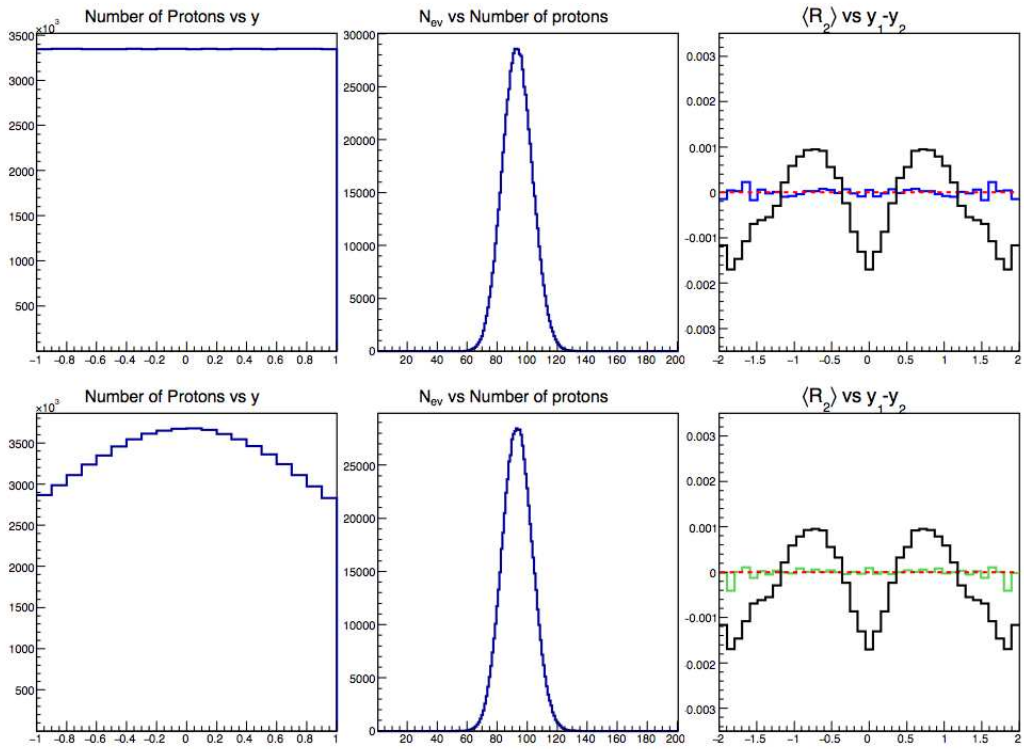

FIG. 7: Top row: calculating $\langle R_2 \rangle$ sampling from flat rapidity distribution and UrQMD N_{part}/evt. Blue $\langle R_2 \rangle$ line is sampling from the distributions. Bottom row: calculating $\langle R_2 \rangle$ sampling from both UrQMD distributions. Green $\langle R_2 \rangle$ is from the sampled distributions. Black $\langle R_2 \rangle$ lines are from UrQMD data.

V. CONCLUSION

Two-particle rapidity dependent correlations for protons in central UrQMD events have been studied using the R2 variable. Multiplicities per event were low enough that a correction for finite counting statistics was needed. UrQMD data shows rapidity dependent correlations for low energies that diminish as the beam energy increases. Sampling randomly from the UrQMD N_{part}/evt and/or rapidity distributions destroys the observed correlations observed in the UrQMD data. Future directions for this analysis include studying other event generator models and applying these techniques to experimental data as well as studying higher dimensional particle correlations (3-particle correlations, 4 particle correlations, etc.).

VI. ACKNOWLEDGEMENTS

This work was performed as part of the 2015 Wayne State University Research Experience for Undergraduates (REU) program funded by the US National Science Foundation. This program was lead by Professors A. Petrov and D. Cinabro. Helpful comments on the present analysis were provided by Professor W.J. Llope, fellow REU participant Kristen Parzuchowski, Professors Sergei Voloshin and Claude Pruneau, and the Wayne State University Relativistic Heavy-Ion group.

VII. BIBLIOGRAPHY

[1] Lawrence Tarini. *Centrality Dependence of two particle Number and Transverse Momentum Correlations in* $\sqrt{S_{NN}}$ *= 200GEV AU + AU Collisions at RHIC* Detroit, Michigan, 2011.

[2] Asis Kumar Chaudhuri. *A Short Course on Heavy Ion Collisions* Bristol: IOP, 2014.

[3] P. Carruthers *Structure of Correlation Functions* Phys. Rev. A Physical Review A 43.6 (1991): 2632-639.

[4] L. Foà *Inclusive Study of High-Energy Multiparticle Production and Two-Body Correlations* CERN. Geneva, Switzerland 1975